Electronic Supplementary Material (ESI) for Analyst.

Supporting Information

Fe-N/C Single-Atom Nanozyme-Based Colorimetric Sensor Array for Discriminating Multiple Biological Antioxidants

Wenjie Jing[a], Xiangkun Cui[b], Fanbo Kong[a], Wei Wei[b,*], Yunchao Li[a], Louzhen Fan[a], Xiaohong Li[a,*]

[a]*Key Laboratory of Theoretical and Computational Photochemistry, Ministry of Education, College of Chemistry, Beijing Normal University, Beijing, 100875, China*

[b]*Department of Chemistry, Capital Normal University, Beijing, 100048,, China*

Email: lxhxiao@bnu.edu.cn

wwei@cnu.edu.cn

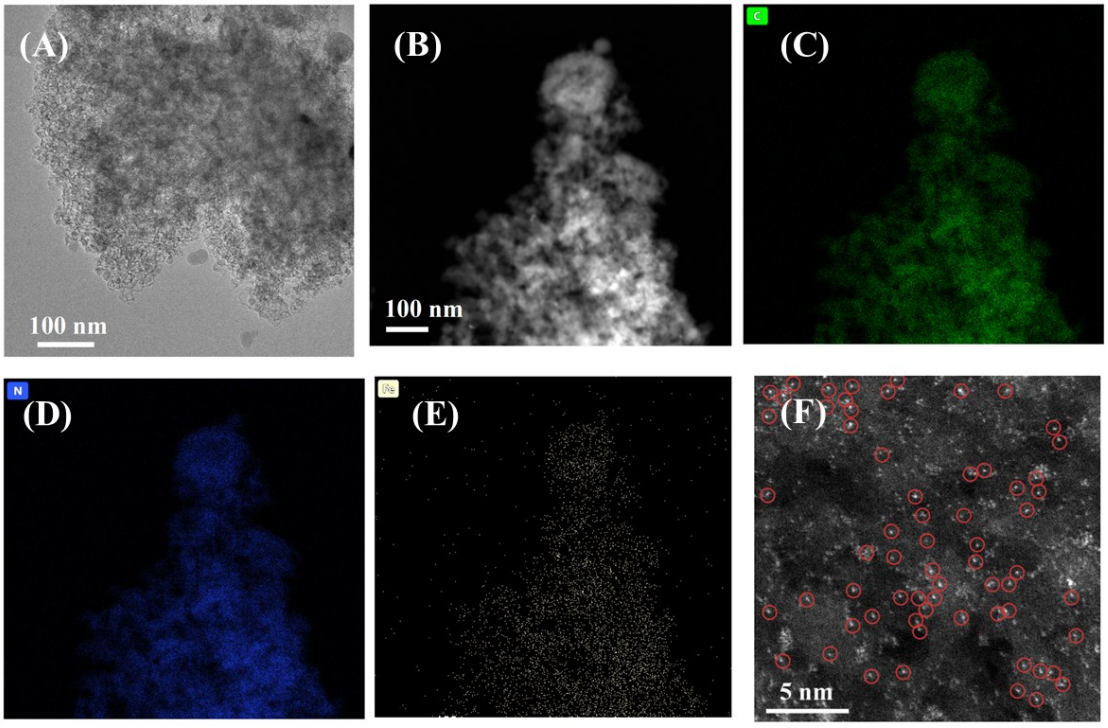

Fig S1. (A) TEM image, (B,C,D,E) STEM image and corresponding elemental mappings of Fe-N/C, (F) HAADF-STEM image of Fe-N/C. Atomically dispersed Fe centers are highlighted by red circles.

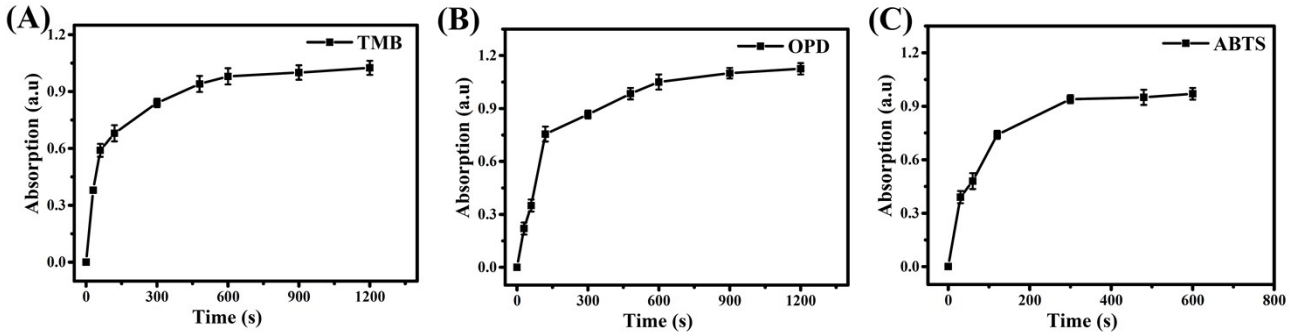

Fig S2. (A) UV/Vis spectra of TMB-Fe-N/C system varies with time, (B) UV/Vis spectra of OPD-Fe-N/C system varies with time, (C) UV/Vis spectra of ABTS-Fe-N/C system varies with time, Error bars represent the standard deviations from at least 3 measurements.

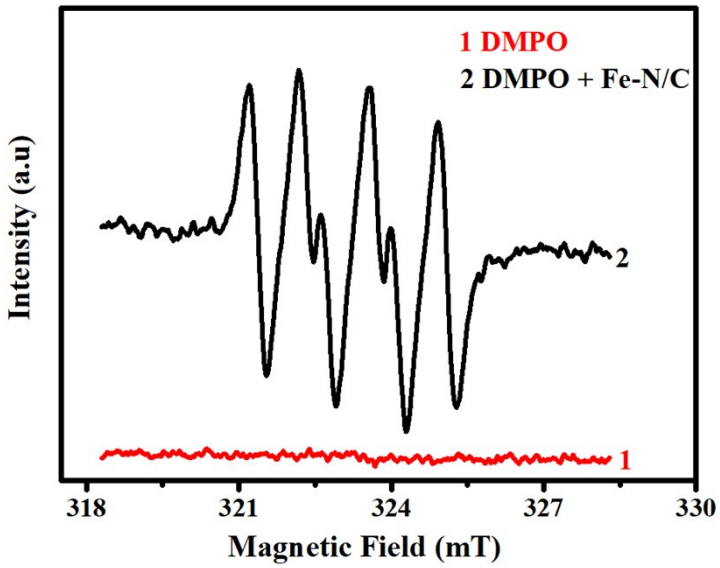

Fig S3. ESR spectra of DMPO and DMPO + Fe-N/C.

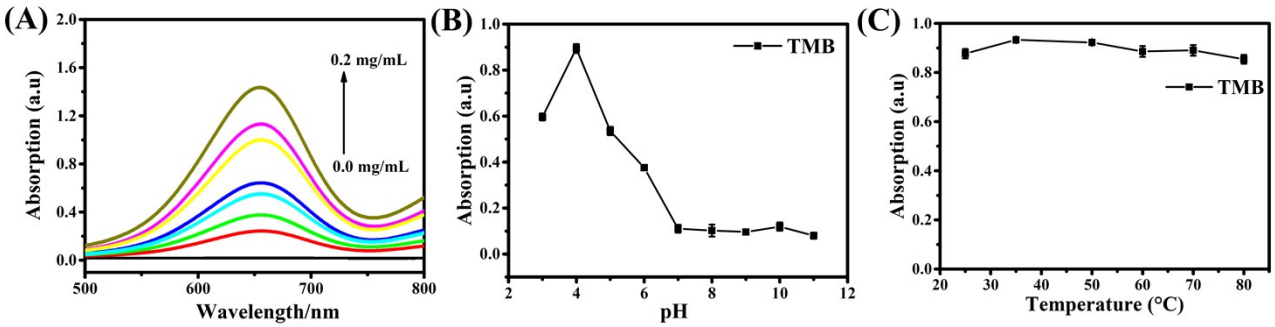

Fig S4. (A) UV-Vis spectra of TMB-Fe-N/C system varies with $C_{Fe\text{-}N/C}$, (B) pH-dependent Oxidase-like property of Fe-N/C with TMB as substrates, (C) temperature-dependent Oxidase-like property of Fe-N/C with TMB as substrates, Error bars represent the standard deviations from at least 3 measurements.

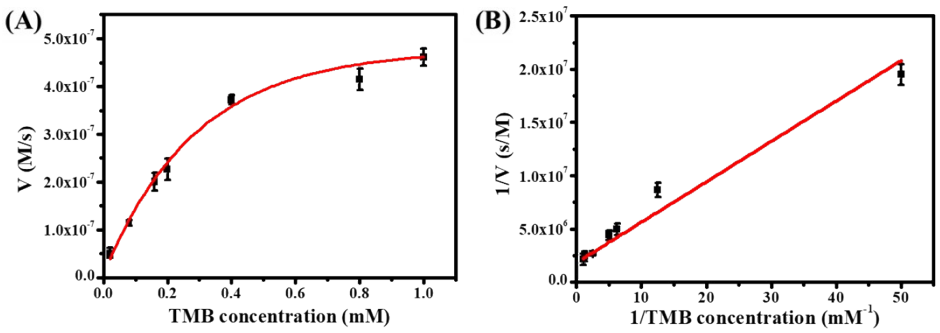

Fig S5. (A) Steady-state kinetic assays of Fe-N/C with TMB as a substrate, (B) the corresponding double reciprocal plots. The concentration of TMB varies from 0.02 mM to 1.0 mM.

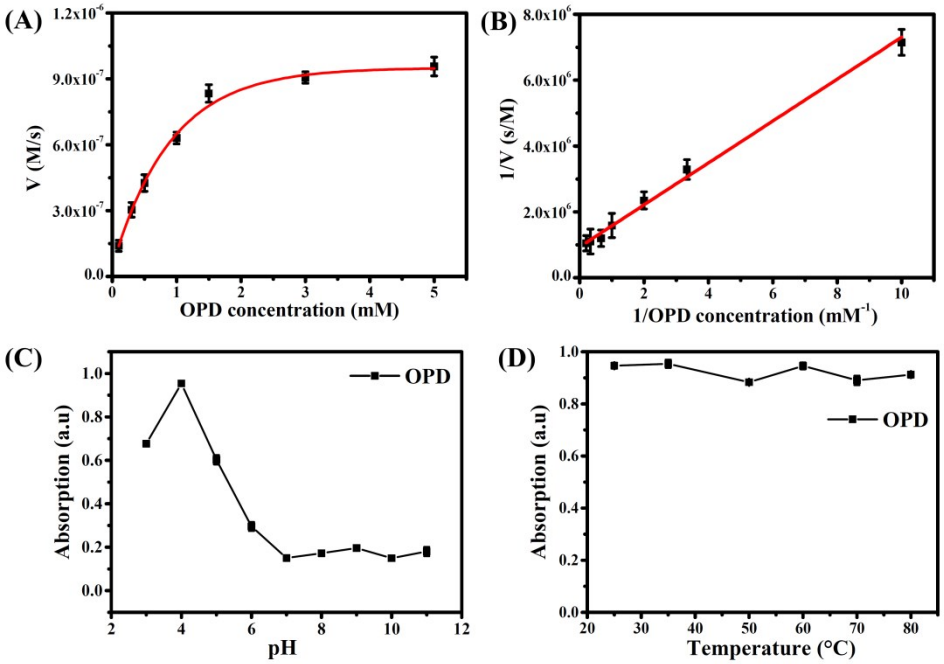

Fig S6. (A) Steady-state kinetic assays of Fe-N/C with OPD as a substrate, (B) the corresponding double reciprocal plots. The concentration of OPD varies from 0.1 mM to 5.0 mM, (C) pH-dependent Oxidase-like property of Fe-N/C with OPD as substrates, (D) temperature-dependent Oxidase-like property of Fe-N/C with OPD as substrates, Error bars represent the standard deviations from at least 3 measurements.

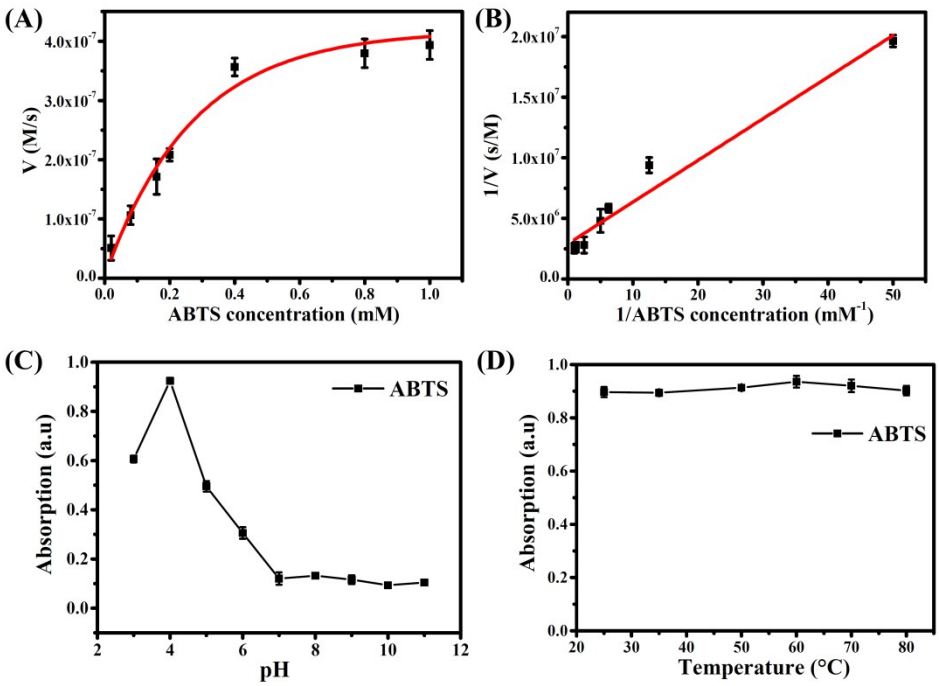

Fig S7. (A) Steady-state kinetic assays of Fe-N/C with ABTS as a substrate, (B) the corresponding double reciprocal plots. The concentration of ABTS varies from 0.02 mM to 1.0 mM, (C) pH-dependent Oxidase-like property of Fe-N/C with ABTS as substrates, (D) temperature-dependent Oxidase-like property of Fe-N/C with ABTS as substrates, Error bars represent the standard deviations from at least 3 measurements.

Table S1. Compared kinetic parameters with other oxidase mimics with TMB as a substrate

Oxidase mimics	K_m (mmol)	V_{max} (mol·L·s^{-1})	Reference
Pt nanoclusters	0.630	2.7×10^{-6}	S1
CeO_2 nanoparticles	0.8-3.8	$1.0\text{-}7.0\times10^{-7}$	S2
Fe_3C/N-Doped	0.225	3.25×10^{-7}	S3
HRP	0.434	1.0×10^{-7}	S4
Fe-N/C	0.205	5.411×10^{-7}	This work

Table S2. Kinetics parameters of Fe-N/C with TMB, OPD and ABTS as substrates.

Substrate	K_m (mmol)	V_{max} (mol·L·s^{-1})	K_{cat} (s^{-1})	*Eff* (mol^{-1}s^{-1})
TMB	0.205	5.411×10^{-7}	5.411×10^{-4}	2.640×10^{-3}
OPD	0.676	1.06×10^{-6}	3.533×10^{-4}	5.226×10^{-4}
ABTS	0.118	3.44×10^{-7}	3.822×10^{-4}	3.239×10^{-3}

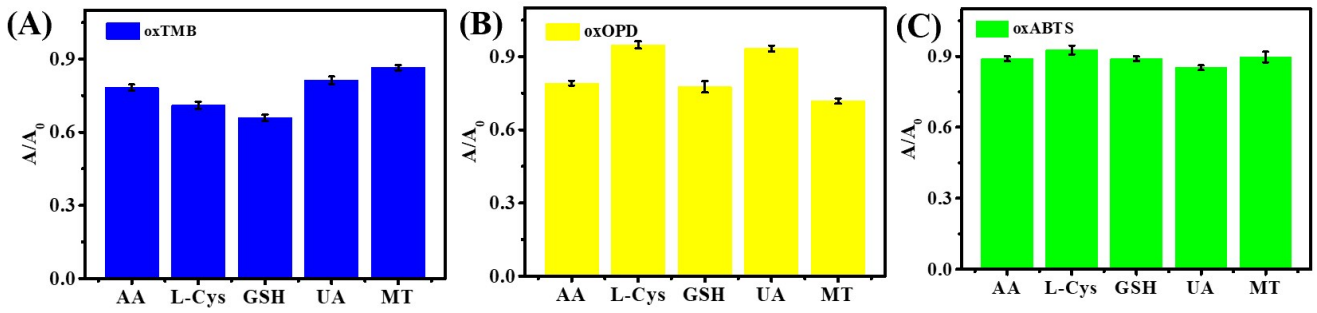

Fig S8. (A) Response of five antioxidants to oxTMB, (B) Response of five antioxidants to oxOPD, (C) Response of five antioxidants to oxABTS, the concentration of each antioxidant was 100 nM. Error bars represent the standard deviations from three replicates.

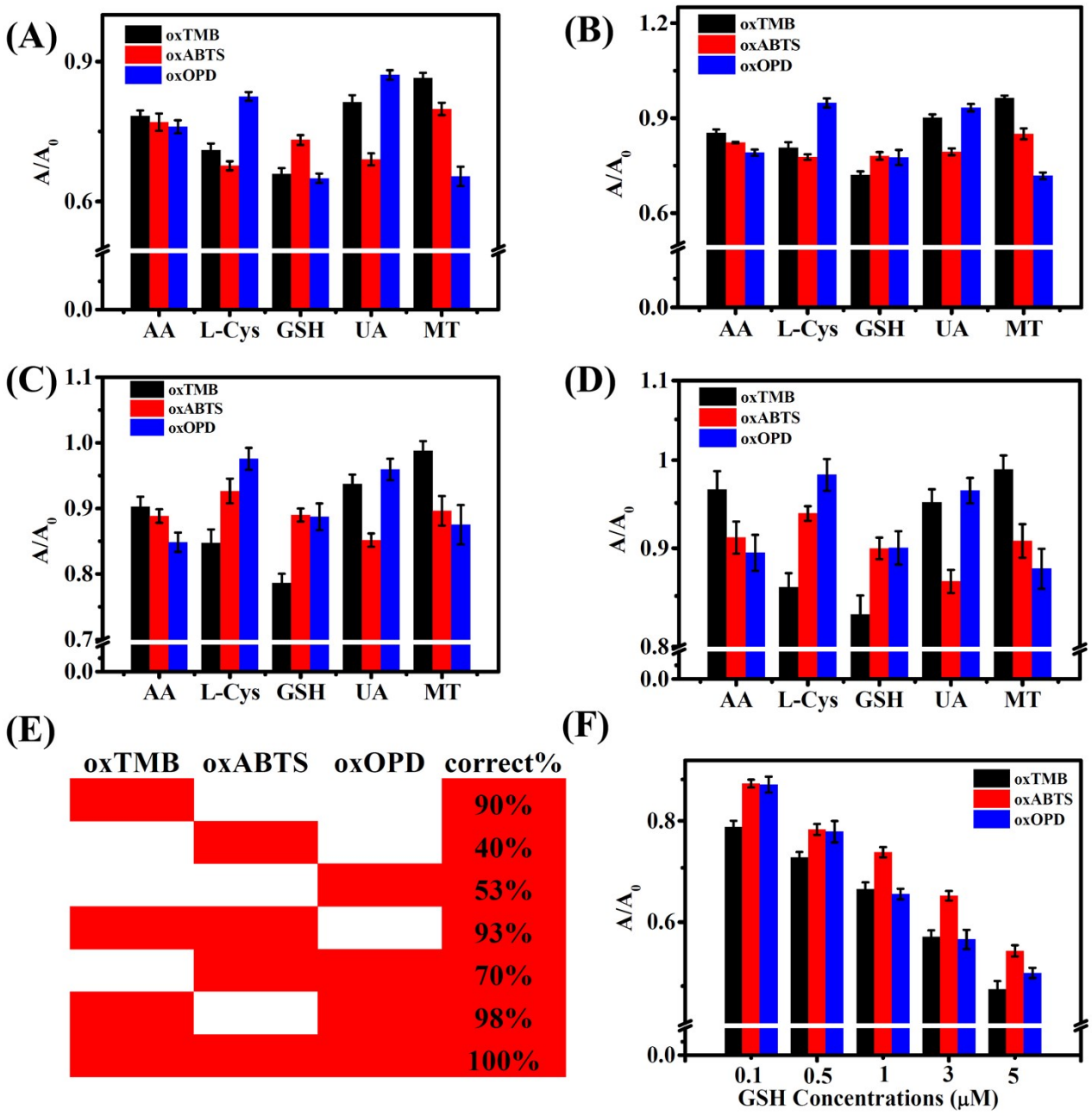

Fig S9. (A) Colorimetric-response patterns (A/A_0) of Fe-N/C Single-Atom Nanozyme sensor arrays toward 1000 nM of antioxidants. (B) Colorimetric-response patterns (A/A_0) of Fe-N/C Single-Atom Nanozyme sensor arrays toward 500 nM of antioxidants. (C) Colorimetric-response patterns (A/A_0) of Fe-N/C Single-Atom Nanozyme sensor arrays toward 100 nM of antioxidants. (D) Colorimetric-response patterns (A/A_0) of Fe-N/C Single-Atom Nanozyme sensor arrays toward 50 nM of antioxidants. (E) Jackknifed classification matrix obtained from three sensing elements for five antioxidants at 100 nM. (F) Colorimetric-response patterns (A/A_0) of Fe-N/C Single-Atom Nanozyme sensor arrays toward various concentrations of GSH. Error bars represent the standard deviations from three replicates.

Table S3. Training matrix of response patterns by three sensing elements against five antioxidants at 1000 nM.

Sample	oxTMB	oxABTS	oxOPD
AA	0.799	0.781	0.744
AA	0.792	0.779	0.741
AA	0.788	0.756	0.772
AA	0.777	0.794	0.767
AA	0.766	0.769	0.771
AA	0.777	0.742	0.765
L-Cys	0.683	0.692	0.830
L-Cys	0.721	0.682	0.815
L-Cys	0.711	0.671	0.819
L-Cys	0.709	0.679	0.839
L-Cys	0.723	0.666	0.817
L-Cys	0.714	0.669	0.830
GSH	0.649	0.734	0.661
GSH	0.672	0.750	0.634
GSH	0.658	0.726	0.646
GSH	0.674	0.726	0.651
GSH	0.658	0.734	0.659
GSH	0.642	0.720	0.647
UA	0.831	0.710	0.867
UA	0.825	0.695	0.860
UA	0.818	0.680	0.871
UA	0.801	0.697	0.882
UA	0.792	0.675	0.885
UA	0.812	0.685	0.862
MT	0.880	0.815	0.625
MT	0.873	0.799	0.631
MT	0.866	0.784	0.671
MT	0.849	0.785	0.673
MT	0.861	0.794	0.665
MT	0.859	0.813	0.656

Table S4. Training matrix of response patterns by three sensing elements against five antioxidants at 500 nM.

Sample	oxTMB	oxABTS	oxOPD
AA	0.867	0.825	0.780
AA	0.854	0.820	0.799
AA	0.840	0.825	0.801
AA	0.863	0.823	0.788
AA	0.840	0.820	0.799
AA	0.855	0.825	0.781
L-Cys	0.797	0.785	0.956
L-Cys	0.832	0.774	0.944
L-Cys	0.825	0.762	0.929
L-Cys	0.799	0.783	0.933
L-Cys	0.788	0.776	0.964
L-Cys	0.799	0.782	0.960
GSH	0.721	0.781	0.809
GSH	0.739	0.799	0.800
GSH	0.714	0.768	0.752
GSH	0.709	0.791	0.762
GSH	0.730	0.769	0.776
GSH	0.714	0.778	0.757
UA	0.916	0.810	0.934
UA	0.910	0.794	0.916
UA	0.903	0.782	0.924
UA	0.895	0.793	0.943
UA	0.897	0.801	0.948
UA	0.890	0.783	0.935
MT	0.970	0.877	0.712
MT	0.963	0.858	0.719
MT	0.956	0.842	0.700
MT	0.951	0.843	0.723
MT	0.972	0.855	0.722
MT	0.965	0.827	0.731

Table S5. Training matrix of response patterns by three sensing elements against five antioxidants at 100 nM.

Sample	oxTMB	oxABTS	oxOPD
AA	0.931	0.879	0.843
AA	0.897	0.894	0.846
AA	0.888	0.904	0.837
AA	0.897	0.890	0.843
AA	0.894	0.876	0.845
AA	0.907	0.887	0.878
L-Cys	0.838	0.938	0.982
L-Cys	0.837	0.900	0.954
L-Cys	0.877	0.907	0.966
L-Cys	0.821	0.929	1.000
L-Cys	0.868	0.937	0.986
L-Cys	0.843	0.948	0.966
GSH	0.808	0.875	0.917
GSH	0.796	0.882	0.898
GSH	0.784	0.899	0.882
GSH	0.777	0.888	0.857
GSH	0.768	0.897	0.878
GSH	0.786	0.898	0.892
UA	0.940	0.861	0.939
UA	0.932	0.836	0.941
UA	0.925	0.851	0.959
UA	0.956	0.863	0.967
UA	0.951	0.844	0.975
UA	0.921	0.855	0.976
MT	0.994	0.872	0.877
MT	0.984	0.877	0.852
MT	0.977	0.881	0.829
MT	0.982	0.913	0.910
MT	1.015	0.908	0.898
MT	0.975	0.926	0.885

Table S6. Identification of blind samples with 100 nM antioxidants.

Sample	oxTMB	oxABTS	oxOPD	Identification	Verification
1	0.771	0.879	0.883	GSH	GSH
2	0.997	0.894	0.856	MT	MT
3	0.888	0.894	0.837	AA	AA
4	0.837	0.920	0.983	L-Cys	L-Cys
5	0.934	0.846	0.945	UA	UA
6	0.787	0.887	0.878	GSH	GSH
7	0.908	0.888	0.832	AA	AA
8	0.927	0.831	0.954	UA	UA
9	0.767	0.907	0.906	GSH	GSH
10	0.821	0.929	1.000	L-Cys	L-Cys
11	0.888	0.877	0.846	AA	AA
12	0.913	0.848	0.966	UA	UA
13	1.008	0.875	0.907	MT	MT
14	0.846	0.912	0.978	L-Cys	L-Cys
15	0.984	0.899	0.882	MT	MT

Table S7. Training matrix of the response patterns for GSH at various concentrations.

C_{GSH}	oxTMB	oxABTS	oxOPD
0.1 μM	0.808	0.875	0.917
0.1 μM	0.796	0.882	0.898
0.1 μM	0.784	0.899	0.882
0.1 μM	0.777	0.888	0.857
0.1 μM	0.768	0.897	0.878
0.1 μM	0.786	0.898	0.892
0.5 μM	0.721	0.781	0.809
0.5 μM	0.739	0.799	0.800
0.5 μM	0.714	0.768	0.752
0.5 μM	0.709	0.791	0.762
0.5 μM	0.730	0.769	0.776
0.5 μM	0.714	0.778	0.757
1 μM	0.649	0.734	0.661
1 μM	0.672	0.750	0.634
1 μM	0.658	0.726	0.646
1 μM	0.674	0.726	0.651
1 μM	0.658	0.734	0.659
1μM	0.642	0.720	0.647
3 μM	0.586	0.655	0.597
3 μM	0.569	0.641	0.584
3 μM	0.559	0.647	0.565
3 μM	0.569	0.638	0.555
3 μM	0.582	0.659	0.566
3 μM	0.585	0.640	0.561
5 μM	0.487	0.563	0.521
5 μM	0.491	0.554	0.515
5 μM	0.501	0.542	0.528
5 μM	0.517	0.542	0.508
5 μM	0.488	0.559	0.526
5 μM	0.490	0.556	0.518

Table S8. Training matrix of the response patterns against the binary mixtures of GSH and MT at different molar ratios (total concentration: 500 nM).

GSH : MT	oxTMB	oxABTS	oxOPD
GSH	0.711	0.781	0.824
GSH	0.709	0.779	0.810
GSH	0.714	0.768	0.792
GSH	0.699	0.751	0.782
GSH	0.710	0.769	0.786
GSH	0.714	0.748	0.806
GSH : MT = 7 : 3	0.744	0.785	0.776
GSH : MT = 7 : 3	0.752	0.784	0.757
GSH : MT = 7 : 3	0.743	0.742	0.739
GSH : MT = 7 : 3	0.726	0.783	0.758
GSH : MT = 7 : 3	0.742	0.800	0.742
GSH : MT = 7 : 3	0.743	0.789	0.742
GSH : MT = 5 : 5	0.835	0.796	0.742
GSH : MT = 5 : 5	0.800	0.796	0.736
GSH : MT = 5 : 5	0.835	0.790	0.721
GSH : MT = 5 : 5	0.833	0.813	0.735
GSH : MT = 5 : 5	0.840	0.800	0.739
GSH : MT = 5 : 5	0.855	0.809	0.740
GSH : MT = 3 : 7	0.886	0.812	0.714
GSH : MT = 3 : 7	0.903	0.806	0.699
GSH : MT = 3 : 7	0.925	0.837	0.714
GSH : MT = 3 : 7	0.897	0.854	0.699
GSH : MT = 3 : 7	0.888	0.831	0.712
GSH : MT = 3 : 7	0.936	0.859	0.721
MT	0.970	0.877	0.682
MT	0.963	0.858	0.689
MT	0.956	0.842	0.680
MT	0.951	0.886	0.693
MT	0.972	0.886	0.702
MT	0.925	0.908	0.681

Table S9. Training matrix of the response patterns against the binary mixtures of MT and L-Cys at different molar ratios (total concentration: 500 nM).

MT : L-Cys	oxTMB	oxABTS	oxOPD
MT	0.970	0.877	0.712
MT	0.963	0.858	0.719
MT	0.956	0.842	0.700
MT	0.951	0.843	0.723
MT	0.972	0.855	0.722
MT	0.965	0.827	0.731
MT : L-Cys = 7 : 3	0.933	0.815	0.795
MT : L-Cys = 7 : 3	0.931	0.808	0.789
MT : L-Cys = 7 : 3	0.924	0.801	0.804
MT : L-Cys = 7 : 3	0.939	0.811	0.805
MT : L-Cys = 7 : 3	0.930	0.799	0.804
MT : L-Cys = 7 : 3	0.925	0.797	0.803
MT : L-Cys = 5 : 5	0.894	0.785	0.856
MT : L-Cys = 5 : 5	0.886	0.774	0.863
MT : L-Cys = 5 : 5	0.903	0.762	0.865
MT : L-Cys = 5 : 5	0.895	0.783	0.860
MT : L-Cys = 5 : 5	0.897	0.776	0.844
MT : L-Cys = 5 : 5	0.888	0.782	0.868
MT : L-Cys = 3 : 7	0.836	0.743	0.914
MT : L-Cys = 3 : 7	0.827	0.755	0.894
MT : L-Cys = 3 : 7	0.831	0.748	0.896
MT : L-Cys = 3 : 7	0.841	0.754	0.906
MT : L-Cys = 3 : 7	0.845	0.736	0.908
MT : L-Cys = 3 : 7	0.838	0.749	0.897
L-Cys	0.797	0.741	0.956
L-Cys	0.782	0.739	0.944
L-Cys	0.785	0.723	0.929
L-Cys	0.799	0.735	0.933
L-Cys	0.788	0.747	0.964
L-Cys	0.799	0.733	0.960

Table S10. Training matrix of the response patterns against the binary mixtures of MT, GSH and L-Cys at different molar ratios (total concentration: 500 nM).

GSH : MT : L-Cys	oxTMB	oxABTS	oxOPD
MT	0.970	0.877	0.682
MT	0.963	0.858	0.689
MT	0.956	0.842	0.680
MT	0.951	0.843	0.693
MT	0.972	0.855	0.702
MT	0.965	0.827	0.681
L-Cys	0.797	0.741	0.956
L-Cys	0.782	0.739	0.944
L-Cys	0.785	0.723	0.929
L-Cys	0.799	0.735	0.933
L-Cys	0.788	0.747	0.964
L-Cys	0.799	0.733	0.960
GSH	0.711	0.781	0.824
GSH	0.709	0.779	0.810
GSH	0.714	0.768	0.792
GSH	0.699	0.751	0.782
GSH	0.710	0.769	0.786
GSH	0.714	0.748	0.806
GSH : MT : L-Cys = 6 : 2 : 2	0.724	0.822	0.735
GSH : MT : L-Cys = 6 : 2 : 2	0.732	0.819	0.764
GSH : MT : L-Cys = 6 : 2 : 2	0.743	0.790	0.742
GSH : MT : L-Cys = 6 : 2 : 2	0.726	0.823	0.743
GSH : MT : L-Cys = 6 : 2 : 2	0.732	0.792	0.730
GSH : MT : L-Cys = 6 : 2 : 2	0.703	0.831	0.769
GSH : MT : L-Cys = 2 : 6 : 2	0.846	0.792	0.724
GSH : MT : L-Cys = 2 : 6 : 2	0.803	0.806	0.699
GSH : MT : L-Cys = 2 : 6 : 2	0.825	0.807	0.734
GSH : MT : L-Cys = 2 : 6 : 2	0.847	0.824	0.709
GSH : MT : L-Cys = 2 : 6 : 2	0.808	0.801	0.732
GSH : MT : L-Cys = 2 : 6 : 2	0.836	0.789	0.721
GSH : MT : L-Cys = 2 : 2 : 6	0.806	0.743	0.824
GSH : MT : L-Cys = 2 : 2 : 6	0.827	0.765	0.834
GSH : MT : L-Cys = 2 : 2 : 6	0.811	0.748	0.796
GSH : MT : L-Cys = 2 : 2 : 6	0.801	0.754	0.826
GSH : MT : L-Cys = 2 : 2 : 6	0.795	0.736	0.818
GSH : MT : L-Cys = 2 : 2 : 6	0.808	0.729	0.777

Table S11. Identification of blind samples with binary mixtures of MT, GSH and L-Cys at different molar ratios (total concentration: 500 nM).

Sample	oxTMB	oxABTS	oxOPD	Identification	Verification
1	0.709	0.779	0.810	GSH	GSH
2	0.956	0.842	0.680	MT	MT
3	0.726	0.823	0.743	GSH : MT : L-Cys = 6 : 2 : 2	6 : 2 : 2
4	0.837	0.920	0.983	L-Cys	L-Cys
5	0.808	0.801	0.732	GSH : MT : L-Cys = 2 : 6 : 2	2 : 6 : 2
6	0.711	0.781	0.824	GSH	GSH
7	0.724	0.822	0.735	GSH : MT : L-Cys = 6 : 2 : 2	6 : 2 : 2
8	0.801	0.754	0.826	GSH : MT : L-Cys = 2 : 2 : 6	2 : 2 : 6
9	0.699	0.751	0.782	GSH	GSH
10	0.799	0.735	0.933	L-Cys	L-Cys
11	0.743	0.790	0.742	GSH : MT : L-Cys = 6 : 2 : 2	6 : 2 : 2
12	0.795	0.736	0.818	GSH : MT : L-Cys = 2 : 2 : 6	2 : 2 : 6
13	0.965	0.827	0.681	MT	MT
14	0.799	0.733	0.960	L-Cys	L-Cys
15	0.846	0.792	0.724	GSH : MT : L-Cys = 2 : 6 : 2	2 : 6 : 2
16	0.811	0.748	0.796	GSH : MT : L-Cys = 2 : 2 : 6	2 : 2 : 6
17	0.836	0.789	0.721	GSH : MT : L-Cys = 2 : 6 : 2	2 : 6 : 2
18	0.970	0.877	0.682	MT	MT

Table S12. Training matrix of response patterns by three sensing elements against 500 nM antioxidants at spiked in human serum.

Sample	oxTMB	oxABTS	oxOPD
AA	0.837	0.797	0.800
AA	0.854	0.832	0.779
AA	0.840	0.825	0.801
AA	0.813	0.799	0.818
AA	0.800	0.788	0.809
AA	0.798	0.799	0.788
L-Cys	0.795	0.761	0.934
L-Cys	0.763	0.749	0.916
L-Cys	0.756	0.724	0.924
L-Cys	0.751	0.739	0.943
L-Cys	0.775	0.730	0.948
L-Cys	0.799	0.724	0.935
GSH	0.712	0.814	0.808
GSH	0.719	0.760	0.810
GSH	0.700	0.816	0.794
GSH	0.723	0.763	0.782
GSH	0.692	0.795	0.793
GSH	0.721	0.793	0.801
UA	0.870	0.829	0.902
UA	0.889	0.818	0.924
UA	0.892	0.825	0.943
UA	0.881	0.792	0.919
UA	0.895	0.791	0.900
UA	0.894	0.826	0.923
MT	0.934	0.825	0.729
MT	0.916	0.830	0.740
MT	0.924	0.825	0.722
MT	0.943	0.823	0.742
MT	0.948	0.840	0.746

MT	0.935	0.855	0.717
Serum	0.194	0.432	0.366
Serum	0.222	0.452	0.323
Serum	0.248	0.420	0.351
Serum	0.184	0.389	0.308
Serum	0.197	0.366	0.285
Serum	0.203	0.408	0.311

Table S13. Identification of blind samples with antioxidants spiked in human serum.

Sample	oxTMB	oxABTS	oxOPD	Identification	Verification
1	0.931	0.849	0.743	MT	MT
2	0.767	0.714	0.946	L-Cys	L-Cys
3	0.888	0.784	0.937	UA	UA
4	0.707	0.810	0.803	GSH	GSH
5	0.914	0.836	0.745	MT	MT
6	0.817	0.787	0.808	AA	AA
7	0.798	0.738	0.912	L-Cys	L-Cys
8	0.837	0.790	0.834	AA	AA
9	0.927	0.827	0.726	MT	MT
10	0.801	0.819	7.800	AA	AA
11	0.868	0.817	0.906	UA	UA
12	0.723	0.788	0.786	GSH	GSH
13	0.808	0.755	0.917	L-Cys	L-Cys
14	0.706	0.782	0.798	GSH	GSH
15	0.884	0.809	0.922	UA	UA

Table S14. Detection results for antioxidants in human serum samples (n = 3).

Sample	Added (nM)	Detected (nM)	Recovery (%)	RSD (%)
Serum	100	93.25	93.25	2.85
	500	510.78	102.16	4.23
	1000	1035.14	103.51	3.57

Additional References

S1 C.-J. Yu, T.-H. Chen, J.-Y. Jiang and W.-L. Tseng, *Nanoscale*, 2014, **6**, 9618-9624.

S2 A. Asati, S. Santra, C. Kaittanis, S. Nath and J. M. Perez, *Angew. Chem. Int. Ed.*, 2009, **48**, 2308-2312.

S3 N. Song, F. Ma, Y. Zhu, S. Chen, C. Wang and X. Lu, *ACS Sustainable Chem. Eng.*, 2018, **6**, 16766-16776.

S4 J. Z. Lizeng Gao, L. Nie, J. Zhang, Y. Zhang, N. Gu, T. Wang,J. Feng, D. Yang, S. Perrett and X. Yan, *Nat. Nanotechnol.,* 2007, **2,** 577-583.